Chapter 16

Methods for Quantitative Analysis of Axonal Cargo Transport

Matias Alloatti, Luciana Bruno, and Tomas L. Falzone

Abstract

Neurons rely on complex axonal transport mechanisms that mediate the intracellular dynamics of proteins, vesicles, and mitochondria along their high polarized structure. The fast improvement of live imaging techniques of fluorescent cargos allowed the identification of the diverse motion properties of different transported molecules. These properties arise as the result of molecular interactions between many players involved in axonal transport. Motor proteins, microtubule tracks, cargo association, and even axonal viscosity contribute to the proper axonal dynamics of different cargos. The unique properties in each cargo determine their distribution and location that is relevant to ensure neuronal cell activity and survival. This chapter provides a computational-based method for the generation of cargo trajectories and the identification of different motion regimes while cargo moves along axons. Then, the procedure to extract relevant parameters from active, diffusive, and confined motion is provided. These properties will allow a better comprehension of the nature and characteristics of cargo motion in living cells, therefore contributing to understanding the consequences of transport defects that arise during diseases of the nervous system.

Key words Axonal transport, Anterograde, Retrograde, Segmental velocities, Run lengths, Pauses, Reversions, Diffusive

1 Introduction

Neuronal connectivity within the brain relies on the distribution of vesicles and proteins that ensure synaptic activity in highly polarized neuronal structures with long extending axons and complex dendrite arborization [1]. In addition, proper retrieval of survival factors and signaling molecules in neurons also depends on a regulated transport system from the periphery to the cytoplasm and nucleus [2]. Therefore, understanding the mechanisms that govern the delivery and presentation of a wide range of proteins and organelles is key to comprehend neuronal function and dysfunction. This knowledge is relevant since early transport defects arise

Stephen D. Skaper (ed.), *Neurotrophic Factors: Methods and Protocols*, Methods in Molecular Biology, vol. 1727,
https://doi.org/10.1007/978-1-4939-7571-6_16,

as crucial intracellular impairments that may lead to the progression of different neurodegenerative diseases [3, 4].

Axonal transport ensures the distribution of cargo through the mechanical force generated by molecular motors along microtubule tracks in an ATP-dependent manner [5]. Due to the axonal microtubule polarity, kinesin motors transport cargos toward the synapses in the anterograde direction, whereas retrograde transport retrieves cargos toward the cell body by the dynein motor complex. Many regulatory steps contribute to cargo transport speed and processivity ranging from microtubule-associated proteins, kinases involved in motor activity regulation, and mechanisms implicated in cargo attachment and detachment from their track [1, 4, 6]. Axonal transport has been studied in a variety of significant models such as live animals, primary cultured neurons, in vitro cellular models, and extruded axons from cephalopods. Recently, human-derived neurons differentiated from pluripotent stem cells open new avenues to understand how transport regulation is achieved and to comprehend the role of transport defects within the human genomic and proteomic background [7–10].

Although it is clear that molecular motors, i.e., kinesin and dynein, are essential for efficient cargo delivery, their coordination is still not completely elucidated [1, 11, 12]. Moreover, microtubule-associated proteins such as tau produce differential effects on the motion of these motors hindering even more our understanding of organelle transport [7, 13–15]. Therefore, the quantitative analysis of cargo trajectories while cargo moves along microtubules has become an essential task to unveil these mechanisms [7, 11, 16, 17]. Typically, single-particle tracking techniques are used to recover the position of fluorescently labeled organelles or vesicles from movies recorded during their transport along the axon [18, 19]. The nature of the driving forces underlying motion can be dissected and classified by the mean square displacement (MSD) that is a measure of the spatial extent of a trajectory along time [20]. Trajectories are then partitioned to retrieve local velocities, run lengths, pauses, and reversal in the direction of motion. Different mechanistic models involving motor competition or coordination can then be confronted to the results of statistical analysis of these quantities, allowing a deeper comprehension of the intracellular transport system [7, 17, 21, 22].

Here, we describe methods to perform imaging acquisition and analysis of fluorescently labeled cargos in polarized neurons. Computational procedures are described to track particles and obtain motion properties such as MSD, segmental velocities, run lengths, pauses, reversions, and diffusion coefficient. Procedures to classify motion regimes depending on the MSD of the trajectory are described. Routines to extract dynamic properties of cargo moving under active transport are presented. Together, these

methods provide a toolbox for the quantitative analysis of cargo trajectories in axons allowing the characterization of transport in control conditions and impairments associated with disease.

2 Materials

2.1 Neuron Cultures

1. Mature and polarized neuronal cell cultures plated over glass coverslips, either from primary neurons or from the differentiation of pluripotent stem cells.
2. Supplemented media used to maintain neurons (*see* **Note 1**).

2.2 Transfection

1. DNA vector driving the expression of protein of interest fused to a fluorescent protein (*see* **Note 2**).

2.3 Imaging

1. Camera with CCD or CMOS technologies providing enough sensitivity to register as fast as 20 ms/frame (Hamamatsu).

2.4 Kymographs, Tracking, and Analysis

1. ImageJ software (https://imagej.nih.gov/ij/index.htm).
2. *MultipleKymograph* plug-in for ImageJ (https://www.embl.de/eamnet/html/body_kymograph.html).
3. MATLAB software (The MathWorks Inc.; *see* **Note 3**).
4. Scripts package for image analysis, downloadable from http://www.ibyme.org.ar/laboratorios/39/transporte-axonal-neurodesarrollo-y-neurodegeneracion.

3 Methods

3.1 Neuron Cultures

1. Axonal transport analysis should be performed in highly polarized neurons (mouse-, rat-, or human-derived) plated on round 35 mm glass bottom coverslips (*see* **Note 4**) in a 24-well plate. Axons should be properly identified.
2. Morphology of axons and dendrites can be identified with immunostainings against tau (total tau or phospho-tau) in combination with microtubule-associated protein 2 [7].
3. Plus-end orientation of microtubules in axons can be confirmed using a microtubule-capping protein such as EB3 in its fluorescent version (EB3-green fluorescent protein). This step is necessary for the correct identification and interpretation of the motor involved in transport and the regulation of cargo movement.

3.2 Transfection of Fluorescent Cargo

1. Transfect neurons with a 1:2 ratio of DNA/Lipofectamine 2000. Neurons in a 24-well plate require 0.8 μg of endotoxin-

free purified DNA diluted in a tube with 50 μL of plain Neurobasal medium. Lipid complexes are mixed by gently dropping 2 μL (1 μg/μL) of Lipofectamine 2000 in 50 μL of Neurobasal medium (without supplements). Incubate at room temperature each individual tube for 5 min. If neurons are plated in different areas or wells, maintain DNA/Lipofectamine ratio.

2. After incubation, combine diluted DNA and Lipofectamine 2000 to reach a total volume of 100 μL. Mix gently, and incubate at room temperature for 20 min.
3. Remove most of the complete medium from the well, and add 100 μL of DNA/Lipofectamine complex (*see* **Note 5**).
4. Incubate 2 h at 37 °C and 5% CO_2, and then replace transfection medium with complete Neurobasal medium (*see* **Note 6**).

3.3 Live Imaging

1. Sixteen to 24 h after transfection, remove the glass with transfected cells from multiwell plates by gently lifting the coverslip with forceps and flipping it over a glass bottom plate containing medium equilibrated in a 5% CO_2 incubator (*see* **Note 7**).
2. Perform live imaging of moving organelles or proteins using a microscope with a heated stage at 37 °C and 5% CO_2 incubation chamber.
3. Identify fluorescent (transfected) cell bodies using a super apochromatic ×100 or ×60 lens. Follow axonal projection at least two fields away from the cell body and two fields away from the axon terminal. It is important to register the position of the cell body and/or the axonal terminal in order to determine motion direction (anterograde or retrograde) of fluorescent particles (Fig. 1a).
4. Register movies using 2 × 2 binning (*see* **Note 8**) according to the fluorescent cargo of interest (Fig. 1b). Register moving cargos at 8–50 frames per second [7, 16]. Save movies in .tiff format.

3.4 Tracking

1. Generate kymographs from movies using ImageJ. Carefully draw a segmented line along the axon in the anterograde direction. Run *MultipleKymograph* plug-in in ImageJ and select line width equal to 3 pixels. Save kymographs as 8bit .tiff files (Fig. 1c).
2. Open MATLAB and track each particle using script A (**tracking_script**; *see* **Notes 9** and **10**). First, select the kymograph of interest. A window opens displaying the kymograph matrix. Track the trajectory placing datatips along its length (*see* **Note 11**). Place more datatips within regions where other trajectories intersect to gain accuracy on single-particle tracking. When the entire trajectory is covered, press mouse's right button and

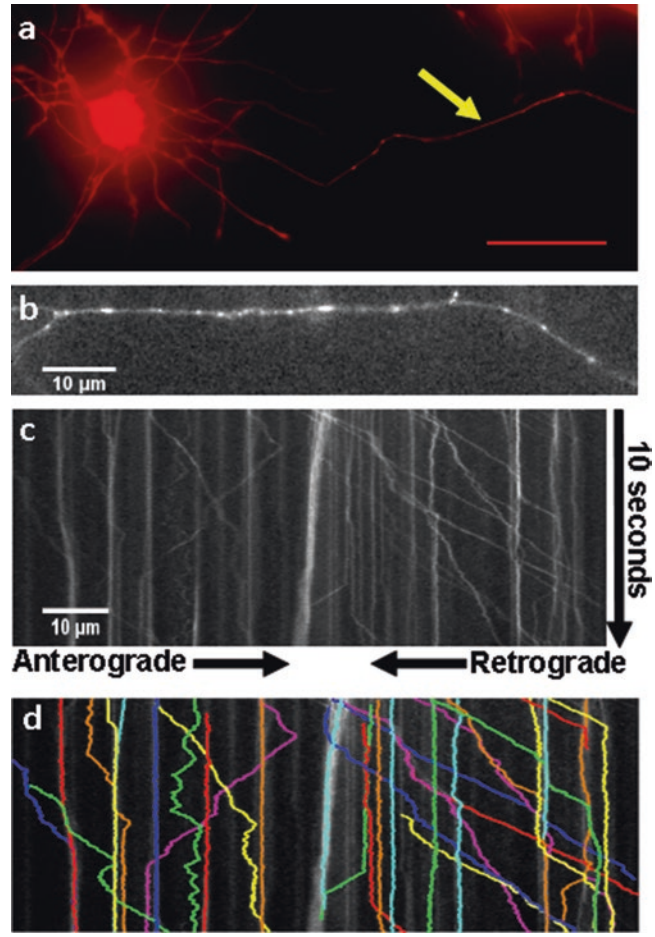

Fig. 1 Trajectories of moving fluorescently labeled cargos identified from kymographs. (**a**) Polarized fluorescent human neuron showing an extending axon (yellow arrow) that can be followed to perform live imaging. (**b**) Snapshot from a high-resolution movie obtained from the axon of a human neuron transfected to visualize amyloid precursor protein vesicles. (**c**) Kymograph of time versus distance obtained from movie shown in (**b**) and oriented in anterograde (right) and retrograde (left) direction. (**d**) Kymograph from (**c**) with colored individual particles identified using tracking_script

export cursor data to workspace. Hit continue button, wait until the program runs, and save the resulting coordinates of the recovered particle.

3. Repeat the procedure to track all trajectories in the kymographs from one experiment (Fig. 1d). Since tracking performance depends on signal to noise ratio, low intensity particles can be difficult to track.

3.5 Data Processing

1. Import all tracks corresponding to an experimental group into MATLAB's workspace (*see* **Note 12**), and run script B-(**MSD_**

script). Script B returns the *MSD* for each trajectory (*see* **Note 13**—Fig. 2a).

2. Save workspace data and run script C (**trajectory_types**). This script classifies trajectories according to their *MSD* in diffusive, confined, or active (Fig. 2b, c). This information is stored in variables *diffusive*, *confined*, and *active*. Each trajectory is identified with numbers within their variable.
3. Active trajectories are associated with motor-dependent transport; arrange and save them in a new MATLAB workspace.
4. To obtain segmental velocities, run script D (**segmental_velocities**) which divides trajectories into segments of 20 frames and returns the mean velocity of each segment (Fig. 2d; *see* **Note 14**). Anterograde and retrograde segmental velocities are stored in *velanterograd*e and *velretrograde* variables, respectively. This data can be exported to a spreadsheet of preference for further comparative and statistical analysis.
5. To extract run lengths, pauses, and reversions, load previous arrangement generated in Subheading 3.5, **step 3**, and run script E (**run lengths_pauses**). This script computes run lengths, pauses, reversions, and complementary data of analyzed trajectories (Fig. 2d).
6. Run length information is condensed in variables *anterograderuns* and *retrograderuns*. These variables contain four columns representing for each uninterrupted segment: velocity (pixels/frames), duration (frames), run length (distance in pixels), and number identifying original trajectory (*see* **Note 15**). Similar information is returned in the variable *pauses*; here, velocity and distance should be approximately zero. The variable *reversions* returns the trajectory label, the frame number where reversion occurred, and the direction of reversion (1 indicates retrograde to anterograde reversions and −1 anterograde to retrograde).

4 Notes

1. Neurobasal medium with 1:50 of 50× B27 supplement and 500 μM L-glutamine is used for primary neurons. Neurobasal medium with 1:100 of 100× N2 supplement, 1:50 of 50× B27 supplement, 1 μg/mL of laminin, 0.1 μM of cyclic AMP, 200 ng/mL of ascorbic acid, 10 ng/mL of brain-derived neurotrophic factor, and 10 ng/mL of glial cell line-derived neurotrophic factor is used for pluripotent stem cell-derived neurons. Store supplemented media at 4 °C.
2. This protocol is intended to image fluorescently fused proteins; therefore, we recommend avoiding the use of dyes. The morphology of neurons can be distinguished by low transfec-

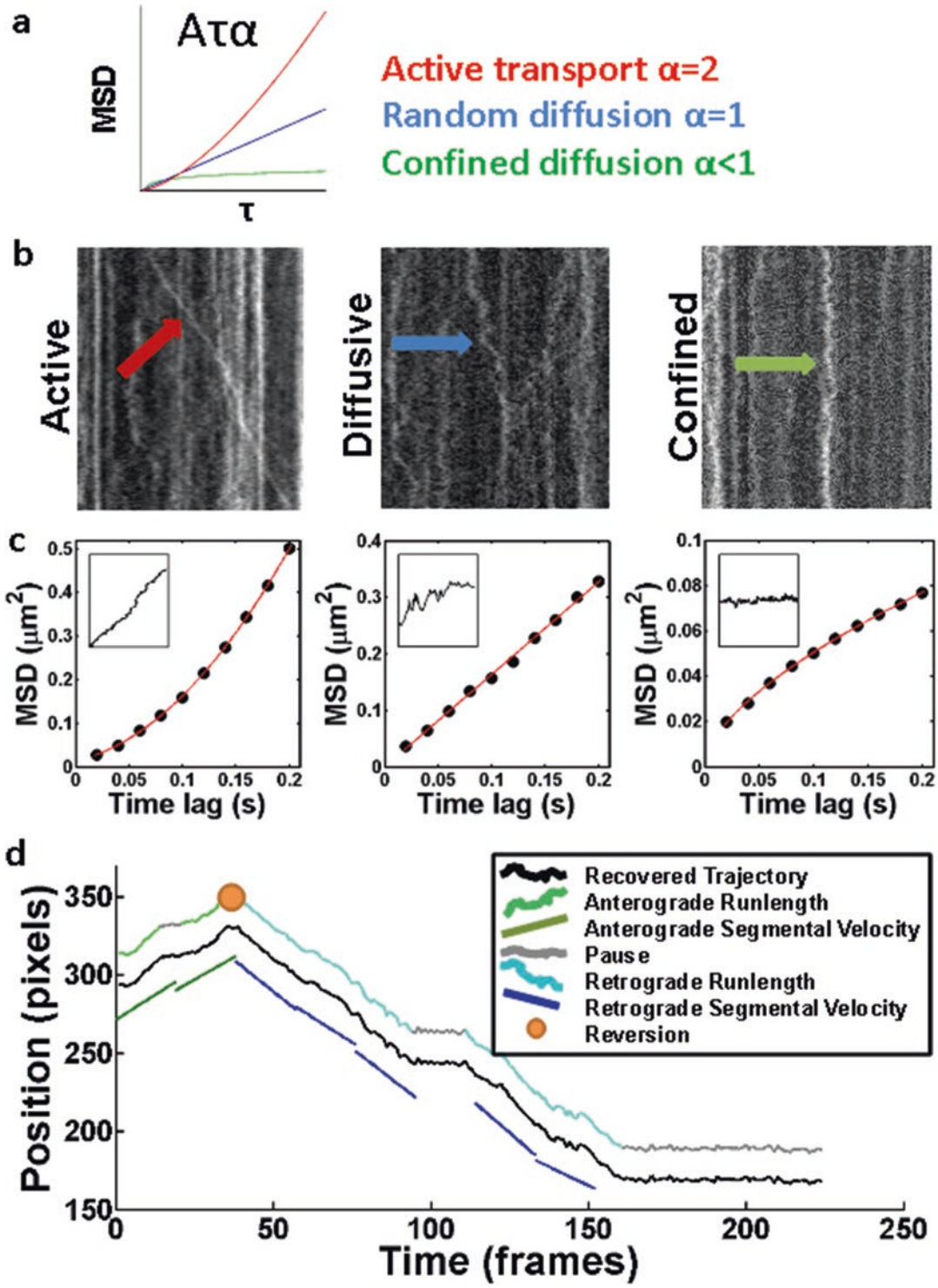

Fig. 2 Transport modes and dynamic properties obtained from detailed quantitative analysis. (**a**) MSD assessed over lag time (τ) indicates the nature of forces contributing to the motion. Trajectories with resulting exponential curves are classified in active transport ($\alpha = 2$), linear curves correspond to diffusive particles ($\alpha = 1$), and logarithmic curves correspond to confined particles ($\alpha < 1$). (**b**) Representative trajectories corresponding to active, diffusive, and confined motion regimes (arrows). (**c**) MSD to τ from the above recovered trajectories displayed also in the inset. (**d**) Single-particle trajectory recovered from tracking is plotted in graph. Motion properties are detailed in the inset as obtained after running script package

tion efficiency, while dyes make it difficult to recognize individual cell orientation.

3. Basic knowledge on MATLAB software environment is required to perform analysis.
4. Glass coverslips (12 mm diameter) are pretreated with nitric acid for 1 h, washed with distilled water three times for 10 min, washed with 95% ethanol three times for 10 min, and again washed with sterile water three times for 10 min. Coat glass with 0.1 mg/mL of poly-L-lysine (30–70 kDa) for 2 h at 37 °C for primary neuronal cultures or with 0.1 mg/mL of poly-L-ornithine (30–70 kDa) overnight and 20 μg/mL of laminin 3 h at 37 °C for pluripotent stem cell-derived neurons.
5. Distribute small drops of medium containing DNA/Lipofectamine complexes at different points of the round coverslip. Make sure medium covers the entire well surface, and rock the plate back and forth.
6. Always remove transfection medium, and add new medium very gently.
7. The sandwich of glass-cells-glass made by flipping the coverslips inside the glass bottom plate (1 mm) allows cells to be in the working distance of high magnification lenses.
8. 2 × 2 binning increases signal intensity and time resolution of imaging but also reduces spatial resolution.
9. Scripts are highlighted in **bold**, and variables in *italics*.
10. An additional file called **readme** provides useful information on how to use the scripts and how to optimize tracking skills.
11. Place datatips in a trajectory from bottom to top. Hold ALT key to generate new datatips, or release and click to reposition the last one generated.
12. Additional script (**Rename_and_prepare**) renames and prepares variables for MSD analysis to be named with an *x* followed by ascending numbers from *1*. This step can be performed manually but is not recommended since it can be quite tedious for large numbers of trajectories.
13. The MSD is a measure of the spatial extent of a trajectory. In 3D, it is defined as

$$\mathrm{MSD}_{(\tau)} = [x_{(t+\tau)} - x_{(t)}]^2 + [y_{(t+\tau)} - y_{(t)}]^2 + [z_{(t+\tau)} - z_{(t)}]^2$$

where t and τ are the absolute and lag times, respectively, and the brackets represent the time average. Assessed over lag time, MSD indicates the nature of the forces contributing to the motion. MSD vs. τ is fitted to the following expression:

$$\mathrm{MSD}_{(\tau)} = \mathrm{MSD}_{(0)} + A\tau^{\alpha}$$

where $MSD_{(0)}$ is a residual value given by the tracking error. The exponent α typically takes values in the range 0–2. Normal diffusion is characterized by $\alpha = 1$ and $A = 6D$, being D the diffusion coefficient. Trajectories with $\alpha > 1.8$, $0.9 < \alpha < 1.1$, or $\alpha < 0.3$ are classified as active, diffusive, or confined, respectively.

14. In script D segments of 20 frames duration are recovered from trajectories and used to compute segmental velocities.
15. Uninterrupted segments in script E are separated by pauses or reversions along a trajectory.

References

1. Maday S, Twelvetrees A, Moughamian A, Holzbaur EF (2014) Axonal transport: cargo-specific mechanisms of motility and regulation. Neuron 84:292–309
2. Ito K, Enomoto H (2016) Retrograde transport of neurotrophic factor signaling: implications in neuronal development and pathogenesis. J Biochem 160:77–85
3. De Vos KJ, Hafezparast M (2017) Neurobiology of axonal transport defects in motor neuron diseases: opportunities for translational research? Neurobiol Dis 105:283
4. Encalada SE, Goldstein LSB (2014) Biophysical challenges to axonal transport: motor-cargo deficiencies and neurodegeneration. Annu Rev Biophys 43:141–169
5. Hirokawa N, Niwa S, Tanaka Y (2010) Molecular motors in neurons: transport mechanisms and roles in brain function, development, and disease. Neuron 68:610–638
6. Brady ST, Morfini GA (2017) Regulation of motor proteins, axonal transport deficits and adult-onset neurodegenerative diseases. Neurobiol Dis 105:273–282
7. Lacovich V, Espindola SL, Alloatti M, Pozo Devoto V, Cromberg LE, Čarná ME, Forte G, Gallo J-M, Bruno L, Stokin GB, Avale ME, Falzone TL (2017) Tau isoforms imbalance impairs the axonal transport of the amyloid precursor protein in human neurons. J Neurosci 37:58–69
8. Pozo Devoto V, Dimopoulous N, Alloatti M, Cromberg L, Otero M, Saez T, Pardi B, Marin-Burgin A, Schinder A, Scassa M, Sevlever G, Falzone T (2017) α-Synuclein control of mitochondrial homeostasis in human-derived neurons is disrupted by mutations associated with Parkinson's disease. Sci Rep 7(1):5042
9. Xu C-C, Denton KR, Wang Z-B, Zhang X, Li X-J (2016) Abnormal mitochondrial transport and morphology as early pathological changes in human models of spinal muscular atrophy. Dis Model Mech 9:39–49
10. Mertens J, Stüber K, Poppe D, Doerr J, Ladewig J, Brüstle O, Koch P (2013) Embryonic stem cell-based modeling of tau pathology in human neurons. Am J Pathol 182:1769–1779
11. Encalada SE, Szpankowski L, Xia CH, Goldstein LS (2011) Stable kinesin and dynein assemblies drive the axonal transport of mammalian prion protein vesicles. Cell 144:551–565
12. Duff K, Knight H, Refolo LM, Sanders S, Yu X, Picciano M, Malester B, Hutton M, Adamson J, Goedert M, Burki K, Davies P (2000) Characterization of pathology in transgenic mice over-expressing human genomic and cDNA tau transgenes. Neurobiol Dis 7:87–98
13. Dixit RRJ, Goldman YE, Holzbaur EL (2008) Differential regulation of dynein and kinesin motor proteins by tau. Science 319:1086–1089
14. Magnani E, Fan J, Gasparini L, Golding M, Williams M, Schiavo G, Goedert M, Amos LA, Spillantini MG (2007) Interaction of tau protein with the dynactin complex. EMBO J 26:4546–4554
15. Perrot R, Julien J-P (2009) Real-time imaging reveals defects of fast axonal transport induced by disorganization of intermediate filaments. FASEB J 23:3213–3225
16. Otero MG, Alloatti M, Cromberg LE, Almenar-Queralt A, Encalada SE, Pozo Devoto VM, Bruno L, Goldstein LS, Falzone TL (2014) Fast axonal transport of the proteasome complex depends on membrane interaction and molecular motor function. J Cell Sci 127:1537–1549
17. Reis GF, Yang G, Szpankowski L, Weaver C, Shah SB, Robinson JT, Hays TS, Danuser G, Goldstein LS (2012) Molecular motor function

in axonal transport in vivo probed by genetic and computational analysis in Drosophila. Mol Biol Cell 23:1700–1714

18. Meijering E, Dzyubachyk O, Smal I (2012) Methods for cell and particle tracking. In: Conn PM (ed) Methods in enzymology. Academic, New York, pp 183–200
19. Gu Y, Sun W, Wang G, Jeftinija K, Jeftinija S, Fang N (2012) Rotational dynamics of cargos at pauses during axonal transport. Nat Commun 3:1030. https://doi.org/10.1038/ncomms2037
20. Gal N, Lechtman-Goldstein D, Weihs D (2013) Particle tracking in living cells: a review of the mean square displacement method and beyond. Rheol Acta 52:425–443
21. Fu MM, Holzbaur EL (2013) JIP1 regulates the directionality of APP axonal transport by coordinating kinesin and dynein motors. J Cell Biol 202:495–508
22. Leidel C, Longoria Rafael A, Gutierrez FM, Shubeita George T (2012) Measuring molecular motor forces in vivo: implications for tug-of-war models of bidirectional transport. Biophys J 103:492–500